

# Hadronic Atoms

J. GASSER<sup>a</sup>, V.E. LYUBOVITSKIJ<sup>b,†</sup> AND A. RUSETSKY<sup>c</sup>

<sup>a</sup> *Center for Research and Education in Fundamental Physics,  
Institute for Theoretical Physics, University of Bern,  
Sidlerstr. 5, CH-3012 Bern, Switzerland*

<sup>b</sup> *Institut für Theoretische Physik, Universität Tübingen,  
Kepler Center for Astro and Particle Physics,  
Auf der Morgenstelle 14, D72076 Tübingen, Germany*

<sup>c</sup> *Helmholtz-Institut für Strahlen- und Kernphysik,  
Bethe Center for Theoretical Physics,  
Universität Bonn, D-53115 Bonn, Germany*

<sup>†</sup> *On leave of absence from: Department of Physics,  
Tomsk State University, 634050 Tomsk, Russia*

**Key Words** QCD, QED, chiral perturbation theory, DGBT formula,  
non-relativistic effective Lagrangians, scattering lengths

## Abstract

We review the theory of hadronic atoms in QCD+QED. The non-relativistic effective Lagrangian approach, used to describe this type of bound states, is illustrated with the case of  $\pi^+\pi^-$  atoms. In addition, we discuss the evaluation of isospin-breaking corrections to hadronic atom observables by invoking chiral perturbation theory.

CONTENTS

Introduction . . . . .	3
Physics background . . . . .	5
The non-relativistic effective theory . . . . .	9
Pionium: Decay of the ground state . . . . .	11
<i>Non-relativistic framework: strong sector</i> . . . . .	12
<i>Including photons</i> . . . . .	15
<i>Bound states</i> . . . . .	18
<i>Scattering lengths</i> . . . . .	22
Pionic hydrogen and pionic deuterium . . . . .	23
Summary points and future issues . . . . .	27

## 1 Introduction

Hadronic atoms are bound states of hadrons, held together predominately by the static Coulomb force. Simple examples are *pionium*, a bound state of two pions with opposite electric charge ( $\pi^+$ ,  $\pi^-$ ), and *pionic hydrogen*, a bound state of a  $\pi^-$  and a proton. Pionium is the analogue of positronium in Quantum Electrodynamics. A more complex example is *pionic deuterium* – a Coulombic bound state of a  $\pi^-$  and a deuteron. The latter itself is a composite state of a proton and a neutron, bound at much smaller distances than the size of the hadronic atom.

The average distance between the constituents of a hadronic atom is given by the Bohr radius

$$r_B = \frac{1}{\alpha\mu_c}, \quad \mu_c = \frac{M_1 M_2}{M_1 + M_2}, \quad (1.1)$$

where  $\alpha \simeq 1/137$  is the fine-structure constant,  $\mu_c$  stands for the reduced mass, and  $M_1, M_2$  are the masses of the constituents. Typically, the Bohr radius is of the order of a few hundred Fermi, much larger than the range of strong interactions. Individual hadrons in the atom spend most of the time at distances where strong interactions are practically absent. For this reason, observables of hadronic atoms are barely affected by the strong interactions.

If the interaction between the constituents were purely electromagnetic and non-relativistic, the energy levels of the atom would be given by the standard quantum-mechanical formula

$$E_n = M_1 + M_2 - \frac{1}{2n^2} \mu_c \alpha^2, \quad n = 1, 2, \dots \quad (1.2)$$

Aside from relativistic corrections which generate higher order terms in  $\alpha$ , this formula is modified in the presence of strong interactions in two ways. First, the energy levels are shifted from their purely electromagnetic value. Furthermore, because the atoms can decay also via strong interactions (example: the decay of pionium into a neutral pion pair through the charge-exchange reaction  $\pi^+\pi^- \rightarrow \pi^0\pi^0$ ), the energy levels are broadened. The effect on the ground-state energy level is illustrated in Fig. 1. The pionium lifetime in the ground state,  $\tau = 1/\Gamma \simeq 3 \times 10^{-15}$  s, is still much smaller than the charged pion lifetime  $\tau_\pi \simeq 10^{-8}$  s. Despite the short lifetime of the atom, the pions travel many times around each other before the atom decays, as the ratio  $\frac{1}{2}\mu_c\alpha^2/\Gamma \simeq 8 \times 10^3$  indicates. As a consequence of this, pionium can be considered a quasi-stable bound state with a clearly defined structure of (almost Coulombic) energy levels. The same

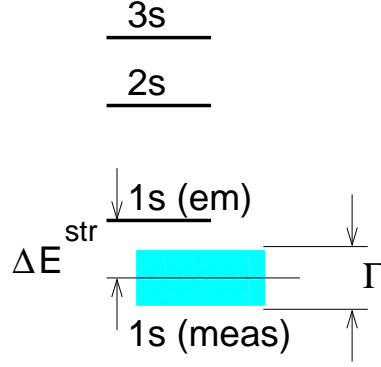


Figure 1: Schematic representation of the shift of the ground state energy level in pionium.  $\Delta E^{\text{str}}$  and  $\Gamma$  denote the strong energy shift and the width in the ground state (we omit indices in  $\Gamma$  throughout, because we will consider the widths of ground states only). The symbols *em* and *meas* denote the purely electromagnetic and the measured energy levels, respectively.

statement is valid for many other hadronic atoms.

Because the size of hadronic atoms is much larger than the range of strong interactions, the energy levels of the atoms can depend only on the characteristics of hadronic interactions at asymptotically large distances. These are usually described in terms of the parameters in the effective range expansion: scattering length, effective range, shape parameters. The situation is analogous to the calculation of the classical static electric field generated by a charge distribution: at asymptotic distances, the electric field depends only on the multipole moments which describe the charge distribution.

Deser, Goldberger, Baumann and Thirring (DGBT) were the first to derive – at leading order in the fine-structure constant  $\alpha$  – a formula for the complex shift of the energy level of a hadronic atom (1). The real and imaginary parts of this shift define the displacement and the width of a given level, generated by the strong interactions. The formula for the ground state reads

$$\Delta E^{\text{str}} - \frac{i}{2}\Gamma = -2\alpha^3\mu_c^2\mathcal{T} + \dots, \quad (1.3)$$

where  $\mathcal{T}$  denotes the complex elastic scattering amplitude of the constituents at the threshold. The ellipses stand for higher order isospin breaking corrections, which will be discussed in detail later in this article. The formula can be trivially generalized to the case of excited energy levels.

The DGBT formula (1.3) plays a central role in the theory of hadronic atoms, because it allows one to extract the threshold amplitude  $\mathcal{T}$  from the experimentally measured energy and width of the atom. Further, the real and imaginary

parts of  $\mathcal{T}$  are related to the hadronic scattering lengths. From this we conclude that the experimental study of hadronic atoms provides us with a source for the determination of these scattering lengths. The above-mentioned huge difference in the atomic and strong interaction scales is very advantageous in the present context, since the atomic observables depend (at leading order) exactly on those quantities (scattering lengths) which one wants to extract from the experiment – they are not sensitive to the short-range details of strong interactions.

In most cases, the first term on the right-hand side of Eq. (1.3) does not match the available experimental precision – next-to-leading order corrections, indicated with the ellipses in Eq. (1.3), are needed as well for a precise determination of the scattering lengths. The aim of any theory of hadronic atoms must be to provide a *systematic* framework for the calculation of these corrections. Here, we will carry out the calculations by using a non-relativistic effective theory of Quantum Chromodynamics + Quantum Electrodynamics (QCD+QED). We will illustrate the method by means of ponium decay, and will briefly consider the application of the same approach to pionic hydrogen and pionic deuterium. We do not discuss quantum-mechanical potential models, because these methods introduce inherent model-dependent artefacts which cannot be controlled.

The article is organized as follows. In section 2 we consider the physics background behind the experiments on various hadronic atoms. In section 3 we briefly discuss the essentials of the non-relativistic effective Lagrangian approach, which is our tool to describe hadronic atoms. Section 4 forms the backbone of the present article. In this section we construct, step by step, the effective field theory approach to ponium decays. The same approach is applied in section 5 to the description of pionic hydrogen and of pionic deuterium. Finally, section 6 contains a brief summary and outlook for future research in the field.

## 2 Physics background

Several experiments with hadronic atoms are presently running. The DIRAC collaboration at CERN is measuring the lifetime of ponium (2, 3, 4, 5, 6, 7, 8) and plans to determine the lifetime of  $\pi K$  atoms as well (9). The Pionic Hydrogen collaboration at PSI (10, 11, 12, 13, 14) studies the spectrum of pionic hydrogen and pionic deuterium, whereas the DEAR/SIDDHARTA collaboration at LNF-INFN (15, 16, 17, 18) plans to determine the ground state energy and width of kaonic hydrogen at a much better accuracy than in previous experiments carried

out at KEK (19, 20). In addition, SIDDHARTA plans the first ever measurement of the spectrum of kaonic deuterium.

These experiments eventually result in a precise determination of various hadronic scattering lengths. Let us recall why the results will be important for the investigation of several fundamental properties of QCD.

1. We start with the DIRAC experiment at CERN (2, 3, 4, 5, 6, 7, 8). The decay width of the ground state of ponium into a  $\pi^0\pi^0$  pair is related to the difference of the  $S$ -wave  $\pi\pi$  scattering lengths  $a_0, a_2$  with total isospin 0 and 2,

$$\Gamma = \frac{2}{9} \alpha^3 p^* (a_0 - a_2)^2 + \dots \quad (2.1)$$

Here,  $p^* = (M_\pi^2 - M_{\pi^0}^2 - \frac{1}{4} M_\pi^2 \alpha^2)^{1/2} + \dots$  is the CM momentum of the neutral pion pair after decay,  $M_\pi, M_{\pi^0}$  are the charged and neutral pion masses, respectively, and the ellipses stand for terms of higher order in isospin breaking.

It is expected that the DIRAC experiment will finally provide a value for  $|a_0 - a_2|$  which is accurate up to a few percent. Other experiments, where the  $\pi\pi$  scattering lengths are determined from  $K_{e4}$  decays (21, 22, 23, 24, 25) or from studying the cusp structures in  $K \rightarrow 3\pi$  decays (26, 27, 28, 29, 30, 31, 32, 33, 34, 35), yield competitive results in terms of accuracy. On the other hand, the difference  $a_0 - a_2$  is particularly sensitive to the value of the quark condensate in QCD (36, 37, 38, 39). In the so-called ‘‘standard’’ scenario which assumes a large condensate, the expansion of the pion mass in terms of the quark mass is

$$M_\pi^2 = M^2 - \frac{\bar{l}_3}{32\pi^2 F^2} M^4 + O(M^6), \quad M^2 = 2\hat{m}B, \quad \hat{m} = \frac{1}{2}(m_u + m_d), \quad (2.2)$$

where the second term on the right hand side of the first equation is small (40). Here,  $F$  is the pion decay constant  $F_\pi$  in the chiral limit,  $m_u, m_d$  are the light quark masses,  $\bar{l}_3$  denotes one of the low-energy constants (LECs) in chiral perturbation theory (ChPT, see, e.g., References (41, 42)), and the quantity  $B$  is related to the quark condensate in the chiral limit (40, 42). Further, if chiral symmetry breaking in QCD proceeds according to the standard picture, a very accurate description of the scattering lengths  $a_0, a_2$  can be achieved by combining 2-loop ChPT with the Roy equations (43, 44),

$$a_0 = 0.220 \pm 0.005, \quad a_2 = -0.0444 \pm 0.0010, \quad a_0 - a_2 = 0.265 \pm 0.004. \quad (2.3)$$

Equipped with this precise theoretical prediction, one may perform a direct experimental test of the chiral symmetry breaking scenario in QCD. Namely, if the measured value of  $a_0 - a_2$  differs significantly from the theoretical prediction,

this would suggest that chiral symmetry breaking proceeds in a manner which is different from the standard scenario. The present situation concerning the verification of the predictions (2.3) is the following. Lattice results for  $a_2$  (45, 46) agree with the prediction within one standard deviation, see Ref. (46) for a compilation of predictions, lattice calculations and data. Due to technical difficulties (disconnected graphs),  $a_0$  has not yet been measured with this technique. On the other hand, using the LECs  $\bar{l}_{3,4}$  (or their  $SU(3) \times SU(3)$  counterparts) determined from the lattice and converting these into a value of  $a_0$  again leads to agreement with the prediction (2.3), within one standard deviation (47, 48, 49, 50, 51, 52, 53). We refer the interested reader to Ref. (48) for discussions and for a review. On the experimental side, data of the DIRAC collaboration on ponium lifetime (7), of NA48/2 on the cusp in  $K \rightarrow 3\pi$  decays (29) and on  $K_{e4}$  events (23) (applying isospin-breaking corrections as described in Refs. (24, 25)) neatly confirm the predictions, although partly still with considerable uncertainties.

2. Next, we briefly consider the proposed measurement of the  $\pi K$  atom lifetime (9), which enables one to extract the value of the isospin-odd  $S$ -wave  $\pi K$  scattering length  $a_0^-$ . The calculations of this scattering length, carried out in ChPT up to two loops, lead to a rather contradictory picture: it turns out (54, 55) that the two-loop contribution to this quantity is apparently larger than the one-loop correction. On the other hand, the result at two loops agrees with the analysis carried out on the basis of Roy equations (56). The situation is puzzling, because, if correct, the convergence of the ChPT series for pion-kaon scattering is under question. It is clear that a precise knowledge of the experimental value of the scattering length is an important ingredient to the solution of this puzzle. For more comments concerning this point, we refer the interested reader to section 2 of the review (57).

3. From the measurement of the pionic hydrogen energy shift and width by the Pionic Hydrogen collaboration at PSI (10, 11, 12, 13, 14), one can extract the isospin even and odd  $S$ -wave  $\pi N$  scattering lengths  $a_{0+}^+$  and  $a_{0+}^-$ . Using Effective Field Theory methods (EFT) in the two-nucleon sector, one can also relate the pion-deuteron scattering lengths to the pion-nucleon ones. [See, e.g., Refs. (58, 59, 60, 61, 62, 63, 64, 65, 66, 67, 68, 69, 70, 71, 72). A similar result can be obtained with quantum-mechanical multiple-scattering theory (see, e.g., Refs. (73, 74, 75)).] Thus, the measurement of the energy shift and width of pionic deuterium results in additional constraints on the values of  $a_{0+}^+$  and  $a_{0+}^-$ .

$\pi N$  scattering lengths are quantities of fundamental importance in low-energy

hadronic physics by themselves, since they test the exact pattern of explicit chiral symmetry breaking. Moreover, knowledge of the exact values of the scattering lengths also affects our understanding of more complicated systems where the  $\pi N$  interaction serves as an input, e.g.  $NN$  interaction, pion-nucleus scattering, three-nucleon forces, etc. In addition, high-precision values of the  $\pi N$  scattering lengths are used as an input for the determination of different basic parameters of QCD at low energies more accurately. One example is the  $\pi NN$  coupling constant  $g_{\pi NN}$ , which is obtained from the Goldberger-Myazawa-Oehme (GMO) sum rule (76, 77, 78), where a particular combination of scattering lengths enters as a subtraction constant. Other important quantities, which can be obtained by using the  $S$ -wave  $\pi N$  scattering lengths as an input, are the so-called pion-nucleon sigma-term and the strangeness content of the nucleon. The sigma-term  $\sigma_{\pi N}$ , which measures the explicit breaking of chiral symmetry in the one-nucleon sector, is defined by

$$\sigma_{\pi N} = \frac{1}{2m_N} \langle ps | \hat{m}(\bar{u}u + \bar{d}d) | ps \rangle, \quad (2.4)$$

where  $|ps\rangle$  denotes a one-nucleon state, with momentum  $p$  and spin  $s$ , and  $m_N$  is the nucleon mass. The sigma-term is related to the strangeness content  $y$  of the nucleon, and to the  $SU(3)$  symmetry breaking part of the strong Hamiltonian,

$$\begin{aligned} \frac{m_s - \hat{m}}{2m_N} \langle ps | \bar{u}u + \bar{d}d - 2\bar{s}s | ps \rangle &= \left( \frac{m_s}{\hat{m}} - 1 \right) (1 - y) \sigma_{\pi N}, \\ y &= \frac{2\langle ps | \bar{s}s | ps \rangle}{\langle ps | \bar{u}u + \bar{d}d | ps \rangle}, \end{aligned} \quad (2.5)$$

where  $m_s$  denotes the strange quark mass. In the analysis of the experimental data, one uses  $S$ -wave  $\pi N$  scattering lengths as input in the dispersion relations, which provide the extrapolation of the isospin even pion-nucleon scattering amplitude from threshold down to the Cheng-Dashen point. We refer the interested reader to Ref. (79) for details. In this reference, the value  $\sigma_{\pi N} \simeq 45$  MeV was obtained. [In Ref. (80), a value for the sigma-term which is considerably larger than 45 MeV is claimed to follow from more recent data.] The sigma-term is rather sensitive to the scattering lengths (79). Consequently, an accurate measurement of the latter will have a large impact on the experimentally determined values of  $\sigma_{\pi N}$  and  $y$ . Finally, we note that the sigma-term is accessible through lattice calculations, see e.g. Ref. (81) and references cited there. It even plays a role in astrophysical applications. As an example for such an impact, we refer the interested reader to the recent publication (82) and the references given there.



4. Last but not least, we discuss the DEAR/SIDDHARTA experiment at LNF-INFN (15, 16, 17, 18). It plans to determine  $\bar{K}N$  scattering lengths from data on kaonic hydrogen and on kaonic deuterium atoms. We believe that it would be very useful to carry out a comparison of the scattering lengths so determined with different theoretical predictions based on the unitarization of the lowest order ChPT amplitude (83, 84, 85, 86, 87, 88, 89, 90, 91). Indeed, it turns out that even the data from kaonic hydrogen alone impose rather stringent constraints on the values of the  $\bar{K}N$  scattering lengths. In some cases, DEAR/SIDDHARTA data seem not to be compatible with the scattering sector (87, 88, 91). It is clear that imposing additional constraints from  $\bar{K}d$  data makes the issue even more pronounced. In our opinion, it is important to check whether the unitarization approach passes this test.

### 3 The non-relativistic effective theory

At leading order, the DGBT formula in Eq. (1.3) is universal: it looks exactly the same in potential scattering theory (where it was derived first) and in quantum field theory. This fact is due to the huge difference between the atomic and the strong interaction scales mentioned in the introduction. On the other hand, the isospin-breaking corrections to this relation, which are due to electromagnetic interactions and to the quark mass difference  $m_d - m_u$ , are not universal. In this article, we describe a systematic theory of hadronic atoms within QCD+QED, which enables one to calculate these corrections in a simple and elegant manner, with an accuracy that matches the experimental precision. [ Because ChPT is the low-energy effective theory of QCD+QED, one might be tempted to start from this framework. However, describing bound states in ChPT by using standard techniques, based on the Bethe-Salpeter equation or on 3-dimensional reductions thereof (92, 93, 94, 95, 96, 97), is a complicated enterprise, which makes it very difficult to reach the required precision. We do not, therefore, discuss this method here.]

Our framework is based on the existence of several different momentum scales in the problem. Counting powers of the fine-structure constant  $\alpha$ , we have to assign the order  $\alpha^0$  to the scale related to the pion mass, because  $M_\pi$  has a non vanishing value also in the absence of electromagnetic interactions. On the other hand, the momentum scale corresponding to atomic phenomena is given by the inverse Bohr radius – i.e., the average 3-momenta inside the atom are  $p_{av} \simeq r_B^{-1} = \alpha\mu_c$ , and

count as order  $\alpha$ . From this one concludes that a *non-relativistic* approach, based on an expansion in (small) momenta, is the appropriate framework to describe hadronic atoms, because the momentum expansion translates into an expansion in the fine-structure constant for hadronic atom observables. The advantage of considering a non-relativistic framework consists in the simple treatment of bound states: they can be described by the Schrödinger equation<sup>1</sup>.

Let us list some very general properties of this approach.

- i) The framework uses the language and methods of (non-relativistic) quantum field theory. In particular, the calculations are based on effective Lagrangians and Hamiltonians.
- ii) The non-relativistic approach allows one to keep the number of heavy particles conserved, by construction. In other words, one always stays within a restricted sector in Fock space.
- iii) The non-relativistic theory describes matrix elements at small external momenta. All high-energy effects – like transitions to sectors with a different number of heavy particles – are encoded in the coupling constants of the effective Lagrangian, which are determined through matching to the underlying theory. In this manner, one makes sure that the effective and the underlying theory are equivalent at low energies.
- iv) *Power counting rules* are at the heart of any effective field theory. The non-relativistic power counting at tree-level amounts to counting the number of space derivatives in various terms. Because each non-relativistic momentum is of order of  $\alpha\mu_c$ , the contributions to the bound-state energy from terms containing higher derivatives are suppressed by additional powers of  $\alpha$ . To carry out calculations of the bound-state energy spectrum at a fixed order in  $\alpha$ , a finite number of terms in the Lagrangian thus suffices [for comparison, in ChPT the number of the relevant terms is infinite].
- v) The non-relativistic Lagrangian is used to generate Feynman graphs in a standard manner. Strong loops respect the power counting, if dimensional regularization is used. Loops with photons can also be made consistent with power counting by applying the so-called *threshold expansion* (99, 100).
- vi) It is useful to extend the power counting to include the isospin break-

---

<sup>1</sup>Caswell and Lepage (98) were the first to use a systematic non-relativistic effective Lagrangian approach to investigate bound states in QED.

ing effects which are generated by the quark mass difference  $m_d - m_u$  as well – along with the electromagnetic corrections characterized by the fine-structure constant  $\alpha$ . There is no strict rule for doing this. We now note that the effect of  $m_d - m_u$  in the pion mass is of order  $(m_d - m_u)^2$ , and linear for kaons and nucleons. It is therefore convenient to introduce a *common* isospin-breaking parameter  $\delta$  and count  $\alpha \sim (m_d - m_u)^2 \sim \delta$  in pionium,  $\alpha \sim (m_d - m_u) \sim \delta$  otherwise. This has the advantage that the leading corrections to the hadronic atom observables, generated by  $\alpha$  and  $m_d - m_u$ , are counted at the same order in  $\delta$ .

vii)) At the end of the day, when the hadronic atom spectrum is calculated and the matching to the underlying theory is performed, there is no reference left to the non-relativistic theory in the final result. The non-relativistic approach is used only at an intermediate stage, in order to facilitate the calculations.

Our main goal here is to *first* evaluate the  $O(\delta)$  isospin-breaking corrections to the leading order strong energy shift and width. These corrections are indicated by the ellipses in the DGBT formula Eq. (1.3). Due to lack of space, we concentrate on those corrections that are relevant for the *width* of the ground state. These are more easy to pin down than those for the real part of the energy shift. In a *second* step, the right hand side of equation Equation (1.3) will be expressed in terms of isospin symmetric scattering lengths, up to isospin breaking corrections. The path to a comparison of the DGBT formula with experimental data is then paved, and a precise determination of scattering lengths becomes feasible.

In the next section, we consider in some detail the construction of a non-relativistic theory along these lines. The framework was developed during the last decade in Refs. (57, 65, 66, 87, 101, 102, 103, 104, 105, 106, 107, 108, 109, 110, 111, 112, 113, 114, 115).

#### 4 Pionium: Decay of the ground state

Instead of presenting the non-relativistic effective theory in its full generality, we have decided to explain the method with one particular example, the decay of pionium. Technical details will be skipped – these can be found, e.g., in Refs. (57, 104, 109). For a thorough discussion of the properties of non-relativistic theories, we refer the reader to Refs. (57, 116).

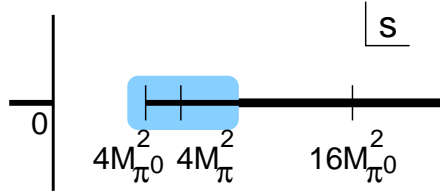


Figure 2: The singularity structure of the  $\pi\pi$  partial-wave scattering amplitudes in the complex  $s$ -plane. The shaded area denotes the low-energy domain.

#### 4.1 Non-relativistic framework: strong sector

We start with a non-relativistic theory for pions, in the absence of photons, which will be included afterwards. On the other hand, it is very convenient to keep from the beginning the masses of charged and neutral pions at their physical values. This is a perfectly consistent procedure, because in the non-relativistic theory, these masses are not renormalized, even when the electromagnetic interactions are turned on.

Our starting point is the relativistic amplitude for the process  $\pi^a(p_1)\pi^b(p_2) \rightarrow \pi^c(p_3)\pi^d(p_4)$ , where  $a, b, c, d = \pm$  or  $0$ . Performing a partial-wave expansion, we arrive at the partial-wave amplitudes that depend on a single Mandelstam variable  $s = (p_1 + p_2)^2$ . Assuming further  $s$  to be a complex variable, we consider the singularity structure of the partial-wave amplitudes in the low-energy region  $|s - 4M_\pi^2| \ll M_\pi^2$  [For definiteness, we consider here the sector with total charge  $Q = 0$ . Other sectors can be discussed analogously.] As it is well known, the partial-wave amplitude is holomorphic in the complex  $s$ -plane, cut along the positive real axis for  $s \geq 4M_{\pi^0}^2$ , see Fig. 2. Another branch point corresponding to the two charged pion threshold is located at  $s = 4M_\pi^2$ , whereas the first inelastic threshold is located at  $s = 16M_{\pi^0}^2$ . In addition, there is a cut on the negative real axis. However, the distance between these faraway singularities and the 2-pion threshold is of the order of the pion mass squared. Consequently, in the low-energy region, which includes the neutral and charged two-pion thresholds (far below the first inelastic threshold), the partial-wave amplitude has a particularly simple form (24),

$$\begin{aligned}
 T_l(s) &= A_l(s) + iB_l(s)\sigma(s) + iC_l(s)\sigma_0(s) + D_l(s)\sigma(s)\sigma_0(s), \\
 \sigma(s) &= \sqrt{1 - \frac{4M_\pi^2}{s}}, \quad \sigma_0(s) = \sqrt{1 - \frac{4M_{\pi^0}^2}{s}}, \quad (4.1)
 \end{aligned}$$

where  $A_l(s), \dots, D_l(s)$  are meromorphic functions in the low-energy domain.

We now present a framework which describes the relativistic  $\pi\pi$  scattering amplitude in the low-energy region, and thus reproduces this structure of the amplitude. The kinetic term in the Lagrangian is fixed through the non-relativistic expansion of the relativistic one-particle energy,

$$\begin{aligned} \mathcal{L}_{kin} &= \sum_{\pm} \Phi_{\pm}^{\dagger} \left( i\partial_t - M_{\pi} + \frac{\Delta}{2M_{\pi}} + \frac{\Delta^2}{8M_{\pi}^3} + \dots \right) \Phi_{\pm} \\ &+ \Phi_0^{\dagger} \left( i\partial_t - M_{\pi^0} + \frac{\Delta}{2M_{\pi^0}} + \frac{\Delta^2}{8M_{\pi^0}^3} + \dots \right) \Phi_0, \end{aligned} \quad (4.2)$$

where  $\Phi_{\pm}, \Phi_0$  denote the non-relativistic field operators for the charged and for neutral pion fields, respectively. The propagator of the non-relativistic charged pion field is given by

$$i\langle 0|T\Phi_{\pm}(x)\Phi_{\pm}^{\dagger}(0)|0\rangle = \int \frac{d^4p}{(2\pi)^4} \frac{e^{-ipx}}{M_{\pi} + \mathbf{p}^2/2M_{\pi} - p^0 - i0}. \quad (4.3)$$

The relativistic corrections due to the higher-order terms in Eq. (4.2) are treated perturbatively. The non-relativistic propagator for the neutral pion is obtained by replacing  $M_{\pi} \rightarrow M_{\pi^0}$ .

The free non-relativistic field operators  $\Phi_{\pm}, \Phi_0$  annihilate the vacuum. This property can be used to construct a theory that – from the beginning – conserves the number of pions. The interaction Lagrangian is then given by an infinite series of 4-pion local operators with an increasing number of space derivatives. In particular, in the 2-particle sector with zero total charge – spanned by the states  $|\pi^+\pi^-\rangle$  and  $|\pi^0\pi^0\rangle$  – the interaction Lagrangian is written as

$$\mathcal{L}_I = c_1 \Phi_+^{\dagger} \Phi_-^{\dagger} \Phi_+ \Phi_- + c_2 (\Phi_+^{\dagger} \Phi_-^{\dagger} \Phi_0 \Phi_0 + \text{h.c.}) + c_3 \Phi_0^{\dagger} \Phi_0^{\dagger} \Phi_0 \Phi_0 + \dots, \quad (4.4)$$

where the ellipses stand for derivative terms. The  $\pi\pi$  scattering amplitude is calculated by using standard Feynman diagram techniques. To be specific, we consider the process

$$\pi^+(p_1)\pi^-(p_2) \rightarrow \pi^+(p_3)\pi^-(p_4). \quad (4.5)$$

Owing to the conservation of the number of pions, the structure of Feynman diagrams is particularly simple: to all orders, the pertinent Green function is determined by the bubble diagrams displayed in Fig. 3. In the CM frame  $P^{\mu} = p_1^{\mu} + p_2^{\mu} = (P^0, \mathbf{0})$ , the contribution from Fig. 3c is proportional to the loop integral

$$\begin{aligned} J(P^0) &= \int \frac{d^4l}{i(2\pi)^4} \frac{1}{M_{\pi} + \mathbf{l}^2/2M_{\pi} - P^0 + l^0 - i0} \frac{1}{M_{\pi} + \mathbf{l}^2/2M_{\pi} - l^0 - i0} \\ &= \frac{iM_{\pi}p_c}{4\pi}; \quad p_c = \sqrt{M_{\pi}(P_0 - 2M_{\pi})}. \end{aligned} \quad (4.6)$$

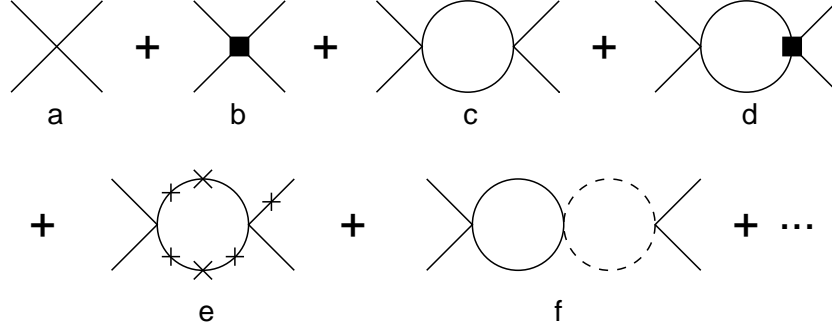


Figure 3: Non-relativistic theory. Typical diagrams which contribute to the two-pion elastic scattering amplitude of the process (4.5). Solid (dashed) lines: charged (neutral) pions. Filled boxes and crosses denote derivative vertices and self-energy insertions, respectively.

We have used dimensional regularization in intermediate steps of the calculation to tame ultraviolet divergences. Neutral pion loops are obtained with the replacement  $M_\pi \rightarrow M_{\pi^0}$ . The contribution to the scattering amplitude for the process Eq. (4.5) is obtained by putting  $P_0 = 2\sqrt{M_\pi^2 + \mathbf{p}^2} = \sqrt{s}$ , where  $\mathbf{p}$  denotes the pion three momentum in the CM frame. Therefore, the bubble graphs in Fig. 3 generate polynomials in the quantities

$$p_c = M_\pi \sigma [1 + O(\sigma^2)], \quad p_0 = M_{\pi^0} \sigma_0 [1 + O(\sigma_0^2)]. \quad (4.7)$$

The so constructed non-relativistic scattering amplitude reproduces the general low-energy structure of the relativistic amplitude in Eq. (4.1). The counterparts of the functions  $A_l(s), \dots, D_l(s)$  are given in form of a power series in  $p_c^2, p_0^2$ , with coefficients that depend on the non-relativistic couplings  $c_1, c_2, c_3, \dots$ .

In order to ensure that the relativistic and the non-relativistic theories describe the same physics at low energies, it remains to *match* the two theories, or, what is the same, to fix the non-relativistic coupling constants  $c_1, c_2, c_3, \dots$ . The matching condition is formulated for the  $T$ -matrix elements,

$$T_R^{ab;cd}(p_1, p_2; p_3, p_4) = [2w_a(\mathbf{p}_1) \cdots 2w_d(\mathbf{p}_4)]^{1/2} T_{NR}^{ab;cd}(p_1, p_2; p_3, p_4), \quad (4.8)$$

where the subscripts  $R$  and  $NR$  label the relativistic and non-relativistic theories, and  $w_a(\mathbf{p}) = \sqrt{M_{\pi^a}^2 + \mathbf{p}^2}$ . The presence of the overall factor in the matching condition (4.8) reflects the difference in the normalization of the one-particle states and the field operator in the non-relativistic and relativistic theories. It is understood that both sides of this equation are expanded in powers of the momenta  $\mathbf{p}_i$ . The matching should therefore be performed at a given order in the momentum expansion – it fixes the polynomial parts of the amplitudes in all

physical channels. This is exactly the freedom one has in choosing the couplings of the non-relativistic Lagrangian. On the other hand, the non-analytic pieces proportional to  $\sigma_c, \sigma_0$  are reproduced automatically, according to analyticity and unitarity, which hold both in the relativistic and in the non-relativistic theories.

This non-relativistic effective theory obeys *power counting rules* in a generic small 3-momentum  $p$ : Bubble diagrams with charged (neutral) pions running in the loop are proportional to  $p_c$  ( $p_0$ ). Consequently, multi-loop diagrams are suppressed by pertinent powers of  $p_c, p_0$ . It can be shown that the relativistic insertions and derivative couplings in the diagrams do not destroy the power counting.

The diagrammatic expansion in this theory coincides with the *effective range expansion*. This can be seen most easily, if one assumes isospin symmetry  $M_\pi = M_{\pi^0}$ . In this case, the bubbles vanish at threshold where  $p_c = p_0 = 0$ , and so do the contributions from the derivative vertices. This means that, to all orders, the threshold amplitudes are determined in terms of the non-derivative couplings  $c_1, c_2, c_3$ . Using the matching condition (4.8), one can express these couplings through the  $\pi\pi$  scattering lengths with definite isospin,

$$\begin{aligned} 3M_\pi^2 c_1 &= 4\pi(2a_0 + a_2) + \cdots, \\ 3M_\pi^2 c_2 &= 4\pi(a_2 - a_0) + \cdots, \\ 3M_\pi^2 c_3 &= 2\pi(a_0 + 2a_2) + \cdots, \end{aligned} \tag{4.9}$$

where the ellipses stand for isospin-breaking corrections. Analogously, the derivative couplings in the Lagrangian can be expressed through effective ranges, shape parameters, etc. This property is ideally suited for describing hadronic atoms: the scattering lengths, which we want to extract from experimental data, turn out to be the parameters of the Lagrangian which will be used to describe the atoms. Consequently, the calculation of atomic observables in perturbation theory by using this Lagrangian will automatically generate a parametrization of the former directly in terms of scattering lengths.

## 4.2 Including photons

The inclusion of virtual photons in this framework is straightforward. First, one follows the paradigm of minimal coupling and replaces ordinary space-time derivatives of the charged pion fields by covariant ones. In addition, the Lagrangian

contains the kinetic term for free photons and a tower of gauge- and rotationally-invariant operators, which can be built from the electric  $\mathbf{E}$  and magnetic  $\mathbf{B}$  fields. For example, the kinetic term for charged pions becomes

$$\mathcal{L}_{kin}^{\pm} = \sum_{\pm} \Phi_{\pm}^{\dagger} \left( iD_t - M_{\pi} + \frac{\mathbf{D}^2}{2M_{\pi}} + \frac{\mathbf{D}^4}{8M_{\pi}^3} + \cdots \mp eh_1 \frac{\mathbf{D}\mathbf{E} - \mathbf{E}\mathbf{D}}{6M_{\pi}^2} + \cdots \right) \Phi_{\pm}, \quad (4.10)$$

where  $D_t\Phi_{\pm} = (\partial_t \mp ieA_0)\Phi_{\pm}$ ,  $\mathbf{D}\Phi_{\pm} = \nabla\Phi_{\pm} \pm ie\mathbf{A}\Phi_{\pm}$  are covariant derivatives,  $e$  is the electric charge, and  $(A_0, \mathbf{A})$  denotes the photon field. Furthermore,  $h_1$  is a new LEC, related to the electromagnetic radius of the pion,  $h_1 = M_{\pi}^2 \langle r_{\pi}^2 \rangle + O(\alpha)$ .

The power-counting at tree-level, which amounts to counting the number of 3-momenta in a given Feynman diagram, can be carried out analogously to the case without photons. However, loop corrections in general lead to a breakdown of naive power-counting rules. This is a well-known problem, caused by the presence of a heavy scale  $M_{\pi}$  in the Feynman integrals: loop integrals receive contributions from regions where the integration momenta are of the order of  $M_{\pi}$ , which cause a breakdown of the counting rules. On the other hand, the effect can be completely removed by simply changing the renormalization prescription in the non-relativistic EFT. This is so because the terms which break power counting behave like polynomials at low energy. Most straightforwardly, the goal can be achieved by modifying the prescription for the evaluation of Feynman integrals. The pertinent modification is called “threshold expansion” (99, 100). A detailed description in the context of the hadronic atom problem can be found, e.g., in Refs. (57, 109). In brief, the method boils down to Taylor-expanding the integrand in any Feynman integral in powers of the 3-momenta prior to performing the loop integrals in dimensional regularization. The expansion and the integration do not commute: it can be shown that the two results differ by just the above-mentioned polynomial contribution, which is absent in the threshold-expanded integral. Thus, applying threshold expansions to all loop integrals leads to a restoration of the naive power counting rules in the non-relativistic EFT.

In principle, the matching condition in the presence of photons is again given by the relation Eq. (4.8). On the other hand, the scattering amplitudes in the presence of real and virtual photons are infrared-divergent in perturbation theory. It is then natural to identify non-singular parts of the amplitude, which are more convenient for matching. At the accuracy needed here, it suffices to discuss the problem at order  $e^2$ , for the charge-exchange process  $\pi^+\pi^- \rightarrow \pi^0\pi^0$ . The structure of the scattering amplitude in the vicinity of the threshold  $|\mathbf{p}| \rightarrow 0$  is



identical in the relativistic and in the non-relativistic case,

$$e^{-i\alpha\theta_c} T^{+-;00} = \frac{e^2 b_1}{|\mathbf{p}|} + e^2 b_2 \ln \frac{2|\mathbf{p}|}{M_\pi} + \mathcal{T}^{+-;00} + O(\mathbf{p}), \quad (4.11)$$

where  $\mathbf{p}$  denotes the relative 3-momentum in the CM frame and  $\theta_c$  is the (infrared-divergent) Coulomb phase,

$$\theta_c = \frac{M_\pi}{2|\mathbf{p}|} \mu^{d-3} \left\{ \frac{1}{d-3} - \frac{1}{2} [\Gamma'(1) + \ln 4\pi] + \ln \frac{2|\mathbf{p}|}{\mu} \right\}. \quad (4.12)$$

The scale  $\mu$  is generated by dimensional regularization, which is used to tame infrared and ultraviolet divergences. The coefficients  $b_{1,2}$  differ by a factor  $4M_\pi^2$  in the relativistic and in the non-relativistic theory. Finally,  $\mathcal{T}^{+-;00}$  denotes the *threshold amplitude*, which is the counterpart of the scattering length in the presence of photons. It is infrared-finite. The matching condition at threshold reads

$$\mathcal{T}_R^{+-;00} = 4M_\pi^2 \mathcal{T}_{NR}^{+-;00}. \quad (4.13)$$

Calculating the diagrams of the type shown in Fig. 4, we arrive at an expression for  $\mathcal{T}_{NR}^{+-;00}$  in terms of the non-relativistic couplings  $c_1, c_2, c_3, \dots$ . At the order of accuracy we are working, only a finite number of diagrams contribute. The final result for the real part of the threshold amplitude is given by

$$\text{Re } \mathcal{T}_{NR}^{+-;00} = 2c_2 - c_2 c_3^2 \frac{\Delta_\pi M_{\pi^0}^2}{2\pi^2} + c_1 c_2 \frac{\alpha M_\pi^2}{4\pi} \left( 1 - \Lambda(\mu) - \ln \frac{M_\pi^2}{\mu^2} \right) + o(\delta), \quad (4.14)$$

where  $\Delta_\pi = M_\pi^2 - M_{\pi^0}^2$ , and  $\Lambda(\mu)$  stands for the *ultraviolet* divergence originating from the diagram in Fig. 4d,

$$\Lambda(\mu) = \mu^{2(d-3)} \left\{ \frac{1}{d-3} - \Gamma'(1) - \ln 4\pi \right\}. \quad (4.15)$$

The ultraviolet divergence is removed in a standard manner, by renormalizing the coupling  $c_2$ .

The matching condition (4.13) enables one to relate a particular combination of the couplings to the relativistic threshold amplitude  $\mathcal{T}_R^{+-;00}$ . At the accuracy needed here, higher-order terms in the momentum expansion of the amplitudes are not needed.

Finally, we note that the non-relativistic couplings  $c_i$  contain both, strong and electromagnetic isospin-breaking corrections. According to the unified counting of the isospin-breaking effects, which was introduced in section 3, we write

$$c_i = \bar{c}_i + \alpha c_i^{(1)} + (m_d - m_u)^2 c_i^{(2)} + o(\delta), \quad (4.16)$$

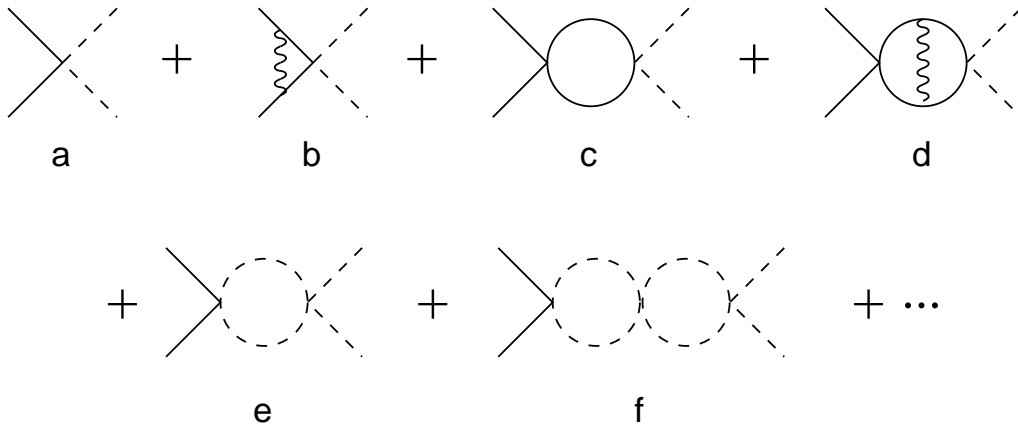


Figure 4: Representative set of diagrams contributing to the scattering amplitude of the process  $\pi^+\pi^- \rightarrow \pi^0\pi^0$  at the order of accuracy we are working. The solid and dashed lines denote charged and neutral pions, respectively, and the wiggled line denotes the Coulomb photon (the calculations are done in the Coulomb gauge). Transverse photons do not contribute at this order. Only the diagrams a,d,f contribute to the expression of the real part of the threshold amplitude, see Eq. (4.14).

where the bar denotes quantities taken in the isospin limit  $\alpha = 0$ ,  $m_d = m_u$ . The  $\bar{c}_i$  can be related to scattering lengths and effective ranges in the isospin symmetric world. On the other hand, the coefficients  $c_i^{(1)}, c_i^{(2)}$  are fixed via matching to ChPT.

### 4.3 Bound states

The non-relativistic framework does not contain any new dynamical information about the behavior of the scattering amplitudes at low momenta, because it is constructed such that it reproduces the relativistic amplitudes. However, the non-relativistic framework is extremely useful when bound states are considered, because methods of standard quantum mechanics can be used to a large extent. As all couplings in the non-relativistic Lagrangian have been fixed through matching of the scattering amplitudes, there are no additional free parameters left in the bound-state sector. Consequently, solving the bound-state problem in the non-relativistic theory, one can eventually express the observables of the bound states in terms of the parameters of the *relativistic* scattering amplitudes. We now describe the procedure.

Hadronic atoms are shallow quasi-stable states formed predominately by the Coulomb force. In order to describe such states, it is convenient to use perturba-

tion theory, where the unperturbed solution corresponds to the purely Coulombic bound state. The full Hamiltonian of the system is constructed from the Lagrangian with standard methods. Here, we concentrate on that part of the Hamiltonian which is responsible for the next-to-leading-order term in the DGBT formula. Moreover, we confine for simplicity the calculation to the *width* of the ground state. As shown in Ref. (109), the pertinent Hamiltonian is

$$\mathbf{H} = \mathbf{H}_0 + \mathbf{H}_C + \mathbf{H}_S + \mathbf{H}_R + \cdots = \mathbf{H}_0 + \mathbf{H}_C + \mathbf{V} + \cdots, \quad (4.17)$$

where  $\mathbf{H}_{0,C,S,R}$  stand for the free non-relativistic Hamiltonian, Coulomb interaction, strong interactions and the relativistic corrections to the pion kinetic energy. [It is convenient to use Coulomb gauge in the non-relativistic calculations. In this gauge, transverse photons can be dropped completely, since they do not contribute at this accuracy to the width. The time-like photon field can be eliminated by using equations of motion, resulting into the static Coulomb potential acting between pions. Finally note that it is legitimate to use different gauges in the relativistic and non-relativistic theories, since only gauge-invariant quantities enter the matching condition.] The ellipses in Eq. (4.17) stand for terms that do not contribute to the width of the ground state at next-to-leading order. The explicit expressions read

$$\begin{aligned} \mathbf{H}_0 &= \int d^3\mathbf{x} \sum_{a=\pm,0} \Phi_a^\dagger(\mathbf{x},0) \left( M_{\pi^a} - \frac{\Delta}{2M_{\pi^a}} \right) \Phi_a(\mathbf{x},0) \\ \mathbf{H}_C &= -\frac{e^2}{4\pi} \int d^3\mathbf{x} d^3\mathbf{y} (\Phi_-^\dagger(\mathbf{x},0)\Phi_-(\mathbf{x},0)) \frac{1}{|\mathbf{x}-\mathbf{y}|} (\Phi_+^\dagger(\mathbf{y},0)\Phi_+(\mathbf{y},0)), \\ \mathbf{H}_S &= \int d^3\mathbf{x} \left\{ -c_1 \Phi_+^\dagger \Phi_-^\dagger \Phi_+ \Phi_- - c_2 (\Phi_+^\dagger \Phi_-^\dagger \Phi_0^2 + \text{h.c.}) - c_3 (\Phi_0^\dagger \Phi_0)^2 \right\}, \\ \mathbf{H}_R &= \int d^3\mathbf{x} \sum_{a=\pm,0} \Phi_a^\dagger(\mathbf{x},0) \left( -\frac{\Delta^2}{8M_{\pi^a}^3} \right) \Phi_a(\mathbf{x},0). \end{aligned} \quad (4.18)$$

It is seen that the Hamiltonian is amazingly simple: it contains three couplings  $c_{1,2,3}$  that need to be matched – all the rest is known.

The pure Coulomb state is an eigenstate of the Hamiltonian  $\mathbf{H}_0 + \mathbf{H}_C$ . The resolvent  $\mathbf{G}_C(z) = (z - \mathbf{H}_0 - \mathbf{H}_C)^{-1}$  develops a tower of poles on the negative real axis in the complex  $z$ -plane, at  $z = E_n = 2M_\pi - \alpha^2 M_\pi / 4n^2$ ,  $n = 1, 2, \dots$  (in the CM frame). The position of these poles coincide with the Coulomb binding energies. Once the perturbation  $\mathbf{V}$  is switched on, the poles move from the real axis to the second Riemann sheet in the complex  $z$ -plane. The energy shift and width of a given state is defined by the real and imaginary parts of the shifted

pole position. Restricting ourselves to the ground state, we write

$$\Delta E - i \frac{\Gamma}{2} = z - E_1, \quad (4.19)$$

The shift  $z - E_1$  of the pole position can be consistently treated with the Feshbach formalism (117, 118). A detailed discussion thereof in the context of hadronic atoms can be found in Refs. (57, 104, 109). There, it is shown that the shift is given by the standard expression known from the Rayleigh-Schrödinger perturbation theory,

$$z - E_1 = \langle \Psi_G | \left\{ \mathbf{V} + \mathbf{V} \sum_{E_\alpha \neq E_1} \frac{|\Psi_\alpha\rangle \langle \Psi_\alpha|}{z - E_\alpha} \mathbf{V} + \dots \right\} | \Psi_G \rangle, \quad (4.20)$$

where the sum over  $\alpha$  runs over both the discrete and continuous spectra of the unperturbed Hamiltonian  $\mathbf{H}_0 + \mathbf{H}_C$ , and  $|\Psi_G\rangle$  denotes the ground-state vector. In momentum space,

$$\Psi_G(\mathbf{k}) = \frac{(64\pi\gamma^5)^{1/2}}{(\mathbf{k}^2 + \gamma^2)^2}, \quad \gamma = 1/r_B = \alpha M_\pi/2. \quad (4.21)$$

The center-of-mass (CM) motion is removed in the above matrix elements, which are then evaluated in the CM frame  $\mathbf{P} = 0$ .

It is instructive to first neglect the relativistic corrections  $\mathbf{H}_R$ . At leading order in  $\mathbf{V}$ , the shift of the pole position is real. Using Eqs. (4.18), (4.20) and (4.21), we get

$$\Delta E = -\frac{\alpha^3 M_\pi^3}{8\pi} c_1 + O(\mathbf{V}^2), \quad \Gamma = O(\mathbf{V}^2). \quad (4.22)$$

The matching condition displayed in Equation (4.9) finally leads to

$$\Delta E = -\frac{1}{6} \alpha^3 M_\pi (2a_0 + a_2) + \dots. \quad (4.23)$$

The ellipses denote contributions of order  $\delta^4$ .

The decay width is of order  $\mathbf{V}^2$ . This leading term is generated by the contribution from the two neutral pion intermediate state in Eq. (4.20). The pertinent threshold is below the bound state energy - these states therefore generate an imaginary part in the energy shift. Since neutral pions do not feel the Coulomb potential, the sum over those intermediate states in Eq. (4.20) merely yields the bubble integral with two neutral pions, similar to the one displayed in Eq. (4.6). The result for the width at this order reads

$$\Gamma = -2 \text{Im } z, \quad (4.24)$$

where  $z$  is a solution to the equation

$$z = -\frac{\alpha^3 M_\pi^3}{4\pi} c_2^2 J_0(z). \quad (4.25)$$

Here,  $J_0(z)$  is given in Eq. (4.6), with  $M_\pi$  replaced by  $M_{\pi^0}$ . The equation (4.25) has a solution on the second Riemann sheet only. The width becomes

$$\Gamma = \frac{\alpha^3 M_\pi^3 M_{\pi^0}}{8\pi^2} \rho^{1/2} c_2^2 + \dots = \frac{2}{9} \alpha^3 \rho^{1/2} (a_0 - a_2)^2 + \dots, \quad (4.26)$$

where  $\rho = 2M_{\pi^0}(M_\pi - M_{\pi^0} - M_\pi \alpha^2/8)$ . In the last step, the matching condition (4.9) was used.

It is seen that the result for the width is of order  $\delta^{7/2}$  at leading order. To work out the next-to-leading order terms, one has to include in Eq. (4.20) contributions up to and including  $\mathbf{V}^3$ , with  $\mathbf{V} = \mathbf{H}_S + \mathbf{H}_R$ . According to power counting, the subsequent terms are suppressed by positive powers of  $\delta$ . This can be seen e.g. from Eqs. (4.6) and (4.7), showing that the charged and neutral bubbles, evaluated at the bound-state energy  $P^0 = E_1$ , count as  $O(\delta)$  and  $O(\delta^{1/2})$ , respectively. This is a very important property of the non-relativistic EFT in dimensional regularization: at a given order in  $\delta$ , only a finite number of terms in the perturbation series contribute.

Finally, the result for the decay width of pionium up to and including terms of order  $\delta^{9/2}$  reads

$$\Gamma = \frac{\alpha^3 M_\pi^3 M_{\pi^0}}{8\pi^2} \rho^{1/2} c_2^2 \left(1 + \frac{5\rho}{8M_{\pi^0}^2}\right) \left(1 - \frac{\rho M_{\pi^0}^2 c_3^2}{4\pi^2}\right) (1 - 2c_1 g(E_1)), \quad (4.27)$$

where  $g(E_1)$  corresponds to the sum of diagrams where any number of Coulomb photons is exchanged between the charged pions. The explicit expression for this quantity is given by

$$g(E_1) = \frac{\alpha M_\pi^2}{8\pi} \left(2 \ln \alpha - 3 + \Lambda(\mu) + \ln \frac{M_\pi^2}{\mu^2}\right). \quad (4.28)$$

Using the matching condition (4.14), one may finally express the decay width through the relativistic threshold amplitude of the process  $\pi^+\pi^- \rightarrow \pi^0\pi^0$ ,

$$\begin{aligned} \Gamma &= \frac{2\alpha^3 p^*}{(32\pi)^2} (\text{Re } \mathcal{T}_R^{+-;00})^2 (1 + K) + o(\delta^{9/2}), \\ K &= \frac{\Delta_\pi}{9M_\pi^2} (a_0 + 2a_2)^2 - \frac{2\alpha}{3} (\ln \alpha - 1) (2a_0 + a_2). \end{aligned} \quad (4.29)$$

We note that the reference to the non-relativistic theory has completely disappeared in the final result Eq. (4.29): the decay width is expressed through the *relativistic* threshold amplitude.

We have thus achieved the first *main goal* mentioned at the end of section 3. It remains to express the relativistic threshold amplitude in terms of isospin symmetric scattering lengths. Then, one can extract these from the measured lifetime of the ponium ground state.

#### 4.4 Scattering lengths

The prediction for the scattering lengths  $a_{0,2}$  in Eq. (2.3) concerns an isospin-symmetric *paradise world* – QCD at  $m_u = m_d$ . In this world, there are no electromagnetic interactions. The light quark masses  $m_u = m_d, m_s$  and the scale  $\Lambda_{QCD}$  are chosen such that  $M_\pi = M_{\pi^+} = 139.57$  MeV,  $M_K = 493.68$  MeV,  $F_\pi = 92.4$  MeV. The precise values of the heavy quark masses  $m_{c,b,t}$  do not matter in the present context. On the other hand, the threshold amplitude, which occurs in the DGBT formula, concerns the real world, where  $m_u \neq m_d, \alpha \neq 0$ . We are thus faced with the problem to relate that amplitude to the scattering lengths evaluated in the paradise world.

The structure of the threshold amplitude at  $\alpha \neq 0, m_u \neq m_d$  is

$$-\frac{3}{32\pi} \text{Re} \mathcal{T}_R^{+-;00} = a_0 - a_2 + h_1(m_d - m_u)^2 + h_2\alpha + o(\delta), \quad (4.30)$$

where the coefficients  $h_i$  can be systematically calculated in the framework of ChPT. These calculations are carried out for the scattering amplitude, not for the bound state observables. Thus, the use of the non-relativistic approach enables one to separate bound state calculations from the chiral expansion.

We outline the determination of  $h_{1,2}$  at order  $p^2$ . The leading order Lagrangian of ChPT is

$$\mathcal{L}_2 = \frac{F^2}{4} \langle \partial_\mu U \partial^\mu U^\dagger + 2B\mathcal{M}(U + U^\dagger) \rangle + C \langle QUQU^\dagger \rangle, \quad (4.31)$$

where the unitary matrix  $U$  contains the pion fields,  $\langle \dots \rangle$  denotes the trace in flavor space, and

$$\mathcal{M} = \text{diag}(m_u, m_d), \quad Q = \frac{e}{3} \text{diag}(2, -1) \quad (4.32)$$

are the quark mass matrix and the charge matrix, respectively. Finally, the constant  $C$  is related to the charged and neutral pion mass difference  $M_\pi^2 - M_{\pi^0}^2 = 2e^2 C/F^2$ .

The threshold scattering amplitude  $\pi^+\pi^- \rightarrow \pi^0\pi^0$  at order  $p^2$  is given by

$$\mathcal{T}_R^{+-;00} = -\frac{s - M_{\pi^0}^2}{F^2} \Big|_{s=4M_\pi^2} = -\frac{3M_\pi^2}{F^2} - \frac{\Delta_\pi}{F^2}. \quad (4.33)$$

From this result, the expressions for  $h_i$  at leading order can be read off,

$$h_1 = O(\hat{m}), \quad h_2 = \frac{3\Delta_\pi}{32\alpha\pi F^2} + O(\hat{m}). \quad (4.34)$$

The details of the calculation at next-to-leading order can be found, e.g., in Refs. (107, 109). The result for the width at next-to-leading order is

$$\Gamma = \frac{2}{9}\alpha^3 p^*(a_0 - a_2)^2(1 + \delta_\Gamma), \quad \delta_\Gamma = (5.8 \pm 1.2) \times 10^{-2}. \quad (4.35)$$

Note that the bulk of the total correction is generated by the leading-order term (4.34), which contains no free parameters. We expect that next-to-next-to-leading corrections will be completely negligible. Vacuum polarization has been investigated in pionium and/or other atoms in References (57, 101, 109, 119, 120).

Using the scattering lengths in Eq. (2.3), we arrive at the prediction for the pionium lifetime (109),

$$\tau = \frac{1}{\Gamma} = (2.9 \pm 0.1) \times 10^{-15} \text{ s}. \quad (4.36)$$

The result of the ongoing measurement carried out by the DIRAC collaboration agrees with this value,

$$\tau = (2.91_{-0.62}^{+0.49}) \times 10^{-15} \text{ s} \quad [\text{DIRAC, Ref. (7)}]. \quad (4.37)$$

It is expected that the precision of the measurement improves in the near future, see Ref. (8).

## 5 Pionic hydrogen and pionic deuterium

The power and beauty of the non-relativistic effective Lagrangian approach is best demonstrated by the fact that the description of *all* hadronic atoms, which were mentioned in the introduction, proceeds very similarly to the pionium case just discussed. On the other hand, some of these bound systems are very different *physically*, and so are the results obtained. The important point is that the language used to describe these systems stays – with only minor modifications – always the same.

As an example, we consider in this section the measurement of the  $S$ -wave  $\pi N$  scattering lengths  $a_{0+}^+$ ,  $a_{0+}^-$  in experiments on pionic hydrogen and pionic deuterium, which are performed by Pionic Hydrogen collaboration at PSI (10, 11, 12, 13, 14). Measuring the energy shift and the width enables one to extract very accurate values of the real and imaginary parts of the elastic  $\pi^- p$  threshold

scattering amplitude, using pretty much the same technique as in the pionium case. Using unitarity and the measured Panofsky ratio finally allows one to extract from data the real part of the threshold amplitudes for both, the elastic  $\pi^-p \rightarrow \pi^-p$  and the charge-exchange  $\pi^-p \rightarrow \pi^0n$  reactions.

In the last step, the threshold amplitudes are again related to the pertinent scattering lengths in the isospin-symmetric world (cf. with subsection 4.4). At leading order, the relation is

$$\begin{aligned} \mathcal{T}^{\pi^-p \rightarrow \pi^-p} &= a_{0+}^+ + a_{0+}^- + \frac{1}{4\pi(1 + M_\pi/m_p)} \left( \frac{4\Delta_\pi}{F_\pi^2} c_1 - \frac{e^2}{2} (4f_1 + f_2) \right), \\ \mathcal{T}^{\pi^-p \rightarrow \pi^0n} &= -a_{0+}^- + \frac{1}{16\pi(1 + M_\pi/m_p)} \left( \frac{g_A^2 \Delta_\pi}{m_p F_\pi^2} + 2e^2 f_2 \right), \end{aligned} \quad (5.1)$$

where  $m_p$  denotes the nucleon mass,  $g_A$  is the axial coupling constant of the nucleon and  $c_1, f_1, f_2$  are various (strong and electromagnetic) LECs from the second-order pion-nucleon Lagrangian (110, 121, 122). (Following the tradition in the literature, we use the same notation for the LEC  $c_1$  as in pionium. We hope that this is not confusing.)

The difference between pionium and pionic hydrogen becomes visible by comparing Eqs. (4.30,4.34) and (5.1): whereas the pertinent isospin-correction for pionium at leading order is parameter-free, Eq. (5.1) contains the LECs  $c_1, f_1, f_2$ , whose values are not established very well. The issue has been discussed in detail in Ref. (57) where, in particular, an update on the values of  $c_1, f_2$  can be found. No reliable determination on the basis of experimental input is available for  $f_1$  at present. This is the reason for a substantial uncertainty in the leading correction in the  $\pi N$  case, which by far exceeds the experimental error in the measurement of the energy shift.

Next, we turn to pionic deuterium, which allows one to extract the pion-deuteron threshold scattering amplitude. However, in this case the analysis is not yet complete: what one intends to finally obtain are the pion-nucleon scattering lengths, which are related to the pion-deuteron amplitude through multiple-scattering theory. This is a very complicated issue, which has been extensively addressed in the past within the framework of potential models. Recently, calculations in EFT have been performed as well (see, e.g., Refs. (58, 59, 60, 61, 62, 63, 64, 65, 66, 67, 68, 69, 70, 71, 72)). This method allows one to largely reduce an uncontrolled systematic error in the resulting values of the  $\pi N$  scattering lengths.

The calculations within EFT have shed new light on the importance of isospin-breaking corrections, a point which is obscure in potential models. Namely, the



pion-deuteron scattering length in the isospin limit vanishes at leading order. For this reason, the isospin-breaking correction to this quantity, determined predominantly by *short-range* physics, turns out to be very large (66). In the context of the pion-nucleon scattering, the same effect has been mentioned in Ref. (123). Further, the isospin-breaking correction to the pion-deuteron threshold amplitude contains the same virtually unknown LEC  $f_1$  as the  $\pi^-p$  elastic scattering amplitude and is therefore determined with a large systematic error.

The experiments on pionic hydrogen and pionic deuterium are complementary to each other. Namely, the data on pionic hydrogen alone determine the scattering lengths  $a_{0+}^+$  and  $a_{0+}^-$  separately. The data on the energy shift of pionic deuterium provides an additional constraint on these two quantities. This can be seen by considering the bands in the  $(a_{0+}^+, a_{0+}^-)$  plane, which correspond to the different observables. Measuring each of the following three observables: the energy shift and width of pionic hydrogen and the energy shift of pionic deuterium fix a particular combination of  $a_{0+}^+$  and  $a_{0+}^-$ . Each combination corresponds to a band, whose width is determined by a combined experimental and theoretical error. If these three bands do not have a common intersection area in the  $(a_{0+}^+, a_{0+}^-)$  plane, then either experiment or/and the theoretical interpretation of the data is not correct.

The consistency check is made complicated by a large uncertainty present in the values of LECs – most notably in  $c_1$  and  $f_1$ . Baru et al. in Ref. (124) have proposed a procedure to partially circumvent the problem. The idea is based on the observation that the LECs  $c_1$  and  $f_1$  enter in the same combination in both, the pionic hydrogen and pionic deuterium energy shift (at leading chiral order). Introducing the quantity

$$\tilde{a}_+ = a_{0+}^+ + \frac{1}{4\pi(1 + M_\pi/m_p)} \left( \frac{4\Delta_\pi}{F_\pi^2} c_1 - 2e^2 f_1 \right), \quad (5.2)$$

it is seen that  $c_1$  and  $f_1$  disappear at leading order from the expressions of the hadronic atom observables, if these are written in terms of  $\tilde{a}_+$  and  $a_{0+}^-$ . Hence, various bands in the plot shown in Fig. 5 are much narrower than the pertinent bands that can be drawn in  $(a_{0+}^+, a_{0+}^-)$  plane (see Ref. (57)). In particular, Fig. 5 demonstrates that three bands still fail to pass this elaborate consistency test. However, it can be argued that next-order isospin-breaking corrections can be large and may change the above picture. In order to carry out a meaningful test, these corrections should be calculated at least to  $O(p^3)$  for all three observables. The possibility to perform the consistency check at higher accuracy, however, is

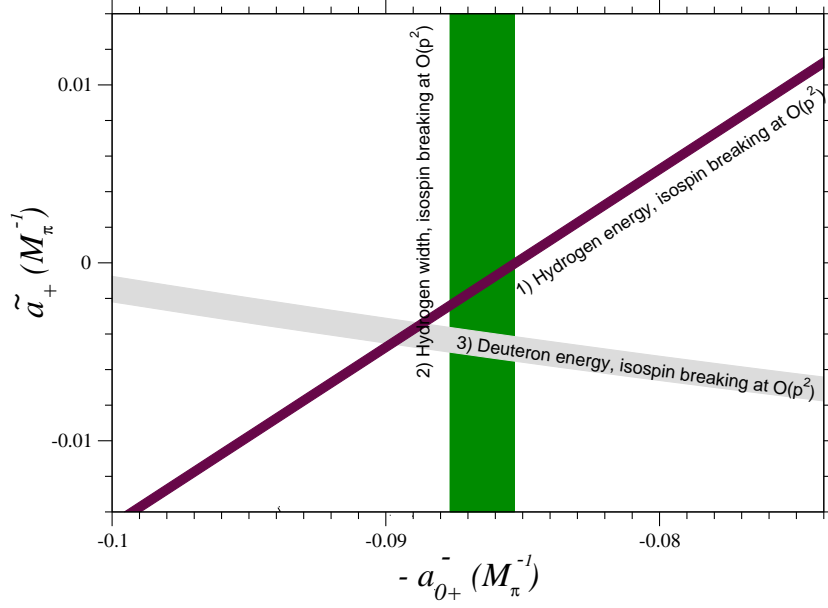


Figure 5: The quantity  $\tilde{a}_+$  defined in Eq. (5.2), plotted against  $a_{0+}^-$ . Three different bands emerge from the measurement of different observables. It is seen that with the isospin breaking corrections evaluated at  $O(p^2)$ , the three bands 1), 2) and 3) have no common intercept.

not yet the end of the story. As it can be seen from Eq. (5.2), the relation of the isospin-symmetric scattering length  $a_{0+}^+$  to the quantity  $\tilde{a}_+$  does contain both,  $c_1$  and  $f_1$ . Thus, in order to determine  $a_{0+}^+$  at a reasonable accuracy, one should find ways to estimate these LECs at the required precision.

Finally, we mention that the extraction of the  $\bar{K}N$  scattering lengths from the experimental data on kaonic hydrogen and kaonic deuterium (15, 16, 17, 18, 19, 20) bears many similarities to the pion-nucleon case. The analysis of the problem within three-flavor ChPT, however, is more complicated due to the large value of the strange quark mass. In addition, the presence of the sub-threshold  $\Lambda(1405)$  resonance leads to a large  $S$ -wave scattering length. As a result, the deuteron problem can no more be treated purely perturbatively, and a partial re-summation of the multiple-scattering series should be considered. These very interesting issues, however, cannot be covered in the present review. The interested reader is referred to the original publications, e.g., Refs. (87, 115, 125, 126, 127, 128).

## 6 Summary points and future issues

- i) Precise data on the energy levels and lifetimes of hadronic atoms enable one to extract various hadronic scattering lengths, provided that a systematic method to work out the relation between data and scattering lengths is available.
- ii) As we discussed in this review, a very convenient framework is provided by the non-relativistic effective Lagrangian approach. Its non-relativistic features are used in intermediate steps only – at the end of the calculations, all observables are expressed in terms of the underlying relativistic theory, QCD+QED.
- iii) Despite the fact that various hadronic atoms observed in Nature are governed by very different underlying physics, the same framework based on the non-relativistic effective Lagrangians applies – with minor modifications – to all of them. This is a beautiful demonstration of the potential and the flexibility of non-relativistic EFT.
- iv) To date, the conceptual problems of the general theory of hadronic atoms have been clarified to a large extent. Now, the focus shifts mainly to applications. Among these, we mention the evaluation of a full set of isospin-breaking corrections at third order in pionic hydrogen and in pionic deuterium. In addition, it would be a major breakthrough to present a systematic calculation of the kaon-deuteron scattering length in terms of the threshold parameters of the  $\bar{K}N$  interaction beyond the static approximation.

### Disclosure statement

The authors are not aware of any biases that might be perceived as affecting the objectivity of this review.

### *Acknowledgments:*

We thank Ulf-G. Meißner for useful comments which helped us to improve the manuscript. The Center for Research and Education in Fundamental Physics is supported by the “Innovations- und Kooperationsprojekt C-13” of the “Schweizerische Universitätskonferenz SUK/CRUS”. This work was supported by the Swiss National Science Foundation, and by EU MRTN-CT-2006-035482

(FLAVIANet). Partial financial support under the EU Integrated Infrastructure Initiative Hadron Physics Project (contract number RII3-CT-2004-506078), by DFG (SFB/TR 16, “Subnuclear Structure of Matter”), by DFG (FA67/31-1, FA67/31-2, GRK683), the President Grant of Russia “Scientific Schools” No. 817.2008.2 and by the Helmholtz Association through funds provided to the virtual institute “Spin and strong QCD” (VH-VI-231) is gratefully acknowledged. One of us (J.G.) is grateful to the Alexander von Humboldt-Stiftung and to the Helmholtz-Gemeinschaft for the award of a prize that allowed him to stay at the HISKP at the University of Bonn, where part of this work was performed. He also thanks the HISKP for the warm hospitality during these stays.

## LITERATURE CITED

1. Deser S, Goldberger ML, Baumann K, Thirring WE. *Phys. Rev.* 96:774 (1954)
2. Afanasev LG, et al. *Phys. Lett.* B338:478 (1994)
3. Adeva B, et al. (DIRAC Collaboration). CERN proposal CERN/SPSLC 95-1 (1995)
4. Halabuka Z, Heim TA, Hencken K, Trautmann D, Viollier RD. *Nucl. Phys.* B554:86 (1999)
5. Adeva B, et al. (DIRAC Collaboration). *J. Phys.* G30:1929 (2004), [hep-ex/0409053](#)
6. Goldin D (DIRAC Collaboration). *Int. J. Mod. Phys.* A20:321 (2005)
7. Adeva B, et al. (DIRAC Collaboration). *Phys. Lett.* B619:50 (2005), [hep-ex/0504044](#)
8. Zhabitsky M (DIRAC Collaboration). [arXiv:0809.4963\[hep-ex\]](#)
9. Adeva B, et al. *Lifetime measurement of  $\pi^+\pi^-$  and  $\pi^\pm K^\mp$  atoms to test low energy QCD*. Addendum to the DIRAC proposal CERN-SPSC-2004-009 [SPSC-P-284 Add.4] (2004)
10. Sigg D, et al. *Phys. Rev. Lett.* 75:3245 (1995)
11. Hauser P, et al. *Phys. Rev.* C58:1869 (1998)
12. Schroder HC, et al. *Eur. Phys. J.* C21:473 (2001)
13. Gotta D (Pionic Hydrogen Collaboration). *Int. J. Mod. Phys.* A20:349 (2005)

14. Simons LM (Pionic Hydrogen Collaboration). *Int. J. Mod. Phys. A*20:1644 (2005)
15. Beer G, et al. (DEAR Collaboration). *Phys. Rev. Lett.* 94:212302 (2005)
16. Zmeskal J, et al. *Nucl. Phys.* A754:369 (2005)
17. Cargnelli M. *Acta Phys. Slov.* 55:7 (2005)
18. Curceanu-Petrascu C, et al. *Eur. Phys. J.* A31:537 (2007)
19. Iwasaki M, et al. *Phys. Rev. Lett.* 78:3067 (1997)
20. Ito TM, et al. *Phys. Rev.* C58:2366 (1998)
21. Rosselet L, et al. *Phys. Rev.* D15:574 (1977)
22. Pislak S, et al. *Phys. Rev.* D67:072004 (2003), [hep-ex/0301040](#)
23. Batley JR, et al. (NA48/2 Collaboration). *Eur. Phys. J.* C54:411 (2008)
24. Colangelo G, Gasser J, Rusetsky A. *Eur. Phys. J.* C59:777 (2009), [arXiv:0811.0775\[hep-ph\]](#)
25. Bloch-Devaux B. *PoS Confinement*8:029 (2009)
26. Budini P, Fonda L. *Phys. Rev. Lett.* 6:419 (1961)
27. Cabibbo N. *Phys. Rev. Lett.* 93:121801 (2004), [hep-ph/0405001](#)
28. Cabibbo N, Isidori G. *JHEP* 0503:021 (2005), [hep-ph/0502130](#)
29. Batley JR, et al. (NA48/2 Collaboration). *Phys. Lett.* B633:173 (2006), [hep-ex/0511056](#)
30. Gamiz E, Prades J, Scimemi I. *Eur. Phys. J.* C50:405 (2007), [hep-ph/0602023](#)
31. Colangelo G, Gasser J, Kubis B, Rusetsky A. *Phys. Lett.* B638:187 (2006), [hep-ph/0604084](#)
32. Bissegger M, Fuhrer A, Gasser J, Kubis B, Rusetsky A. *Phys. Lett.* B659:576 (2008), [arXiv:0710.4456\[hep-ph\]](#)
33. Abouzaid E, et al. (KTeV Collaboration). *Phys. Rev.* D78:032009 (2008), [arXiv:0806.3535\[hep-ex\]](#)
34. Bissegger M, Fuhrer A, Gasser J, Kubis B, Rusetsky A. *Nucl. Phys.* B806:178 (2009), [arXiv:0807.0515\[hep-ph\]](#)
35. Kampf K, Knecht M, Novotny J, Zdrahal M. *Nucl. Phys. Proc. Suppl.* 186:334 (2009), [arXiv:0810.1906\[hep-ph\]](#)

36. Fuchs NH, Sazdjian H, Stern J. *Phys. Lett.* B269:183 (1991)
37. Stern J, Sazdjian H, Fuchs NH. *Phys. Rev.* D47:3814 (1993),  
hep-ph/9301244
38. Knecht M, Moussallam B, Stern J, Fuchs NH. *Nucl. Phys.* B457:513 (1995),  
hep-ph/9507319
39. Knecht M, Moussallam B, Stern J, Fuchs NH. *Nucl. Phys.* B471:445 (1996),  
hep-ph/9512404
40. Colangelo G, Gasser J, Leutwyler H. *Phys. Rev. Lett.* 86:5008 (2001),  
hep-ph/0103063
41. Weinberg S. *Physica* A96:327 (1979)
42. Gasser J, Leutwyler H. *Ann. Phys.* 158:142 (1984)
43. Colangelo G, Gasser J, Leutwyler H. *Phys. Lett.* B488:261 (2000),  
hep-ph/0007112
44. Colangelo G, Gasser J, Leutwyler H. *Nucl. Phys.* B603:125 (2001),  
hep-ph/0103088
45. Beane SR, Bedaque PF, Orginos K, Savage MJ (NPLQCD Collaboration).  
*Phys. Rev.* D73:054503 (2006), hep-lat/0506013
46. Beane SR, Luu TC, Orginos K, Parreno A, Savage MJ, Torok A, Walker-Loud A. *Phys. Rev.* D77:014505 (2008), arXiv:0706.3026[hep-lat]
47. Del Debbio L, Giusti L, Luscher M, Petronzio R, Tantalo N. *JHEP* 0702:056  
(2007), hep-lat/0610059
48. Leutwyler H. *Proc. Chiral Dynamics, Theory and Experiment,*  
*Durham/Chapel Hill*, p. 17. Singapore: World Scientific (2007),  
hep-ph/0612112
49. Boucaud P, et al. (ETM Collaboration). *Phys. Lett.* B650:304 (2007),  
hep-lat/0701012
50. Bernard C, et al. *PoS LAT2007:090* (2007), arXiv:0710.1118[hep-lat]
51. Kadoh D, et al. (PACS-CS Collaboration). *PoS LAT2007:109* (2007),  
arXiv:0710.3467[hep-lat]
52. Allton C, et al. (RBC-UKQCD). *Phys. Rev.* D78:114509 (2008),  
arXiv:0804.0473[hep-lat]
53. Noaki J, et al. (JLQCD and TWQCD Collaboration). *Phys. Rev. Lett.*  
101:202004 (2008), arXiv:0806.0894[hep-lat]

54. Bijnens J, Dhonte P, Talavera P. *JHEP* 0405:036 (2004), [hep-ph/0404150](#)
55. Schweizer J. *Phys. Lett.* B625:217 (2005), [hep-ph/0507323](#)
56. Büttiker P, Descotes-Genon S, Moussallam B. *Eur. Phys. J.* C33:409 (2004), [hep-ph/0310283](#)
57. Gasser J, Lyubovitskij VE, Rusetsky A. *Phys. Rept.* 456:167 (2008), [arXiv:0711.3522\[hep-ph\]](#)
58. Weinberg S. *Phys. Lett.* B295:114 (1992), [hep-ph/9209257](#)
59. Beane SR, Bernard V, Lee TSH, Meißner UG. *Phys. Rev.* C57:424 (1998), [nucl-th/9708035](#)
60. Beane SR, Savage MJ. *Nucl. Phys.* A717:104 (2003), [nucl-th/0204046](#)
61. Borasoy B, Griesshammer HW. *Int. J. Mod. Phys.* E12:65 (2003)
62. Beane SR, Bernard V, Epelbaum E, Meißner UG, Phillips DR. *Nucl. Phys.* A720:399 (2003), [hep-ph/0206219](#)
63. Baru V, Hanhart C, Kudryavtsev AE, Meißner UG. *Phys. Lett.* B589:118 (2004), [nucl-th/0402027](#)
64. Doring M, Oset E, Vicente Vacas MJ. *Phys. Rev.* C70:045203 (2004), [nucl-th/0402086](#)
65. Meißner UG, Raha U, Rusetsky A. *Eur. Phys. J.* C41:213 (2005), [nucl-th/0501073](#)
66. Meißner UG, Raha U, Rusetsky A. *Phys. Lett.* B639:478 (2006), [nucl-th/0512035](#)
67. Epelbaum E. *Prog. Part. Nucl. Phys.* 57:654 (2006), [nucl-th/0509032](#)
68. Platter L, Phillips DR. *Phys. Lett.* B641:164 (2006), [nucl-th/0605024](#)
69. Valderrama MP, Arriola ER. [nucl-th/0605078](#)
70. Lensky V, Baru V, Haidenbauer J, Hanhart C, Kudryavtsev AE, Meißner UG. *Phys. Lett.* B648:46 (2007), [nucl-th/0608042](#)
71. Hanhart C. [arXiv:nucl-th/0703028](#)
72. Baru VA, Haidenbauer J, Hanhart C, Kudryavtsev AE, Lensky V, Meißner UG. *Phys. Lett.* B659:184 (2008), [arXiv:0706.4023\[nucl-th\]](#)
73. Thomas AW, Landau RH. *Phys. Rept.* 58:121 (1980)
74. Ericson TEO, Weise W. *Pions and Nuclei*. Oxford: Clarendon (1988)
75. Deloff A. *Phys. Rev.* C64:065205 (2001), [nucl-th/0104067](#)

76. Goldberger ML, Miyazawa H, Oehme R. *Phys. Rev.* 99:986 (1955)
77. Ericson TEO, Loiseau B, Thomas AW. *Phys. Rev.* C66:014005 (2002),  
hep-ph/0009312
78. Abaev VV, Metsa P, Sainio ME. *Eur. Phys. J.* A32:321 (2007),  
arXiv:0704.3167 [hep-ph]
79. Gasser J, Leutwyler H, Sainio ME. *Phys. Lett.* B253:252 (1991)
80. Pavan MM, Strakovsky II, Workman RL, Arndt RA. *PiN Newslett.* 16:110  
(2002), hep-ph/0111066
81. Ohki H, et al. (JLQCD Collaboration). *Phys. Rev.* D78:054502 (2008),  
arXiv:0806.4744 [hep-lat]
82. Asano M, Matsumoto S, Senami M, Sugiyama H. *Phys. Lett.* B663:330  
(2008), arXiv:0711.3950 [hep-ph]
83. Kaiser N, Siegel PB, Weise W. *Nucl. Phys.* A594:325 (1995),  
nucl-th/9505043
84. Oset E, Ramos A. *Nucl. Phys.* A635:99 (1998), nucl-th/9711022
85. Oller JA, Meißner UG. *Phys. Lett.* B500:263 (2001), hep-ph/0011146
86. Jido D, Oller JA, Oset E, Ramos A, Meißner UG. *Nucl. Phys.* A725:181  
(2003), nucl-th/0303062
87. Meißner UG, Raha U, Rusetsky A. *Eur. Phys. J.* C35:349 (2004),  
hep-ph/0402261
88. Borasoy B, Nissler R, Weise W. *Phys. Rev. Lett.* 94:213401 (2005),  
hep-ph/0410305
89. Borasoy B, Nissler R, Weise W. *Eur. Phys. J.* A25:79 (2005),  
hep-ph/0505239
90. Oller JA, Prades J, Verbeni M. *Phys. Rev. Lett.* 95:172502 (2005),  
hep-ph/0508081
91. Borasoy B, Meißner UG, Nissler R. *Phys. Rev.* C74:055201 (2006),  
hep-ph/0606108
92. Lyubovitskij VE, Rusetsky A. *Phys. Lett.* B389:181 (1996),  
hep-ph/9610217
93. Jallouli H, Sazdjian H. *Phys. Rev.* D58:014011 (1998),  
[Erratum-ibid.D58:099901(1998)], hep-ph/9706450



94. Lyubovitskij VE, Lipartia EZ, Rusetsky AG. *Pisma Zh. Eksp. Teor. Fiz.* 66:747 (1997), [JETPLett.66:783(1997)], hep-ph/9801215
95. Ivanov MA, Lyubovitskij VE, Lipartia EZ, Rusetsky AG. *Phys. Rev.* D58:094024 (1998), hep-ph/9805356
96. Sazdjian H. *Phys. Lett.* B490:203 (2000), hep-ph/0004226
97. Jallouli H, Sazdjian H. *Eur. Phys. J.* C48:561 (2006), hep-ph/0605253
98. Caswell WE, Lepage GP. *Phys. Lett.* B167:437 (1986)
99. Kinoshita T, Nio M. *Phys. Rev.* D53:4909 (1996), hep-ph/9512327
100. Beneke M, Smirnov VA. *Nucl. Phys.* B522:321 (1998), hep-ph/9711391
101. Labelle P, Buckley K. hep-ph/9804201
102. Kong X, Ravndal F. *Phys. Rev.* D59:014031 (1999)
103. Holstein BR. *Phys. Rev.* D60:114030 (1999), nucl-th/9901041
104. Gall A, Gasser J, Lyubovitskij VE, Rusetsky A. *Phys. Lett.* B462:335 (1999), hep-ph/9905309
105. Kong X, Ravndal F. *Phys. Rev.* D61:077506 (2000), hep-ph/9905539
106. Eiras D, Soto J. *Phys. Rev.* D61:114027 (2000), hep-ph/9905543
107. Gasser J, Lyubovitskij VE, Rusetsky A. *Phys. Lett.* B471:244 (1999), hep-ph/9910438
108. Lyubovitskij VE, Rusetsky A. *Phys. Lett.* B494:9 (2000), hep-ph/0009206
109. Gasser J, Lyubovitskij VE, Rusetsky A, Gall A. *Phys. Rev.* D64:016008 (2001), hep-ph/0103157
110. Gasser J, Ivanov MA, Lipartia E, Mojžiš M, Rusetsky A. *Eur. Phys. J.* C26:13 (2002), hep-ph/0206068
111. Schweizer J. *Phys. Lett.* B587:33 (2004), hep-ph/0401048
112. Schweizer J. *Eur. Phys. J.* C36:483 (2004), hep-ph/0405034
113. Schweizer J. *Int. J. Mod. Phys.* A20:358 (2005), hep-ph/0408055
114. Zemp P. PhD thesis (University of Bern, 2004)
115. Meißner UG, Raha U, Rusetsky A. *Eur. Phys. J.* C47:473 (2006), nucl-th/0603029
116. Antonelli V, Gall A, Gasser J, Rusetsky A. *Annals Phys.* 286:108 (2001), hep-ph/0003118

117. Feshbach H. *Ann. Phys.* 5:357 (1958)
118. Feshbach H. *Ann. Phys.* 19:287 (1962)
119. Karshenboim S, Jentschura U, Ivanov V, Soff G. *Eur. Phys. J.* D2:209 (1998)
120. Eiras D, Soto J. *Phys. Lett.* B491:101 (2000), [hep-ph/0005066](#)
121. Fettes N, Meißner UG, Steininger S. *Nucl. Phys.* A640:199 (1998), [hep-ph/9803266](#)
122. Müller G, Meißner UG. *Nucl. Phys.* B556:265 (1999), [hep-ph/9903375](#)
123. Weinberg S. *Trans. New York Acad. Sci.* 38:185 (1977)
124. Baru V, Haidenbauer J, Hanhart C, Kudryavtsev AE, Lensky V, Meißner UG. *Proc. 11th Int. Conf. on Meson-Nucleon Physics and the Structure of the Nucleon (MENU2007)*, Juelich (2007), [arXiv:0711.2743\[nucl-th\]](#)
125. Dalitz RH, Tuan SF. *Annals Phys.* 8:100 (1959)
126. Dalitz RH, Tuan SF. *Annals Phys.* 10:307 (1960)
127. Deloff A, Law J. *Phys. Rev.* C20:1597 (1979)
128. Kamalov SS, Oset E, Ramos A. *Nucl. Phys.* A690:494 (2001), [nucl-th/0010054](#)